Viscoplasticity and finite elements for landslide analysis

Viscoplasticité et éléments finis pour l'analyse des glissements de terrains

L.VULLIET, Department of Civil Engineering and Engineering Mechanics, University of Arizona, Tucson, USA
C.S.DESAI, Department of Civil Engineering and Engineering Mechanics, University of Arizona, Tucson, USA

SYNOPSIS: An advanced elasto- viscoplastic model is presented. It incorporates the plasticity model of Desai and coworkers (the hierarchical approach) in the viscoplastic framework of Perzyna. A finite element formulation is derived and the algorithm is given in detail. Two theoretical case studies are treated, illustrating the solution procedure and comparing plastic and viscoplastic solutions. The model is finally used in the case of the "La Frasse" landslide, showing how the proposed model can be advantageously used for analyzing slowly moving soil masses.

INTRODUCTION

Time dependent phenomena in soil mechanics can be roughly grouped in three categories: consolidation, creep and combination of both. The first group has been extensively studied; here the time dependent behavior is conditioned by the seepage characteristics and the compressibility of the soil skeleton; as a first approximation the fluid compressibility may be neglected as well as the viscosity of both constituents (fluid and solid). Usually, a simple constitutive model for the soil skeleton is used (linear or nonlinear elasticity) but generalization to elastoplasic models is straightforward.

Creep phenomena were first studied in the context of secondary consolidation (volumetric creep) and creep of slopes (mainly deviatoric creep). However, most of the advanced studies in this field concern metals at high temperatures (see a review and evaluation in Inoue, 1987). These results may be applied to soil mechanics to some extent as we will do in this paper. The last category (coupling of viscous behavior and consolidation) is a challenging area that has rarely been touched without extreme simplifications. We will be concerned here by the second group only.

There are several different ways of incorporating time-effects in a constitutive model. The integral description is one possibility; the Volterra-Boltzmann equation of hereditary creep (viscoelasticity) is another example and more recent theories like the endochronic theory (Valanis, 1971) may be seen as an extension of this approach.

The other, more frequently used description is the differential approach. A single constitutive equation suffices to describe what is often referred as "creeping materials", for example a relation between the strain rate and the stress (see a review of these and other models for soils under slow movements in Vulliet and Hutter, 1988). Additional equations are needed to describe visco-plastic materials.

A "hardening visco-plastic material" is described by a rate independent yield surface, a viscous flow rule and an elastic constitutive equation for stress. Such a material is suitable for soils under slow strain rates (quasi-static loading). One important member of this group is the Pezyna's model (Perzyna, 1966); it has been applied to soil mechanics problems by different authors (see Desai and Zhang, 1987).

ELASTO-VISCOPLASIC MODEL

Perzyna's theory of visco-plasticity is very similar to the usual plasticity. The basic ingredients will be summarized hereafter for the small strain situation. The symbolic notation is used; bold letters represent vectors and matrices.

The total strain tensor $\boldsymbol{\epsilon}$ is additively decomposed into an elastic part $\boldsymbol{\epsilon}^e$ and a viscoplastic part $\boldsymbol{\epsilon}^{vp}$:

$$\dot{\boldsymbol{\epsilon}} = \dot{\boldsymbol{\epsilon}}^e + \dot{\boldsymbol{\epsilon}}^{vp} \tag{1}$$

The idea here is to incorporate both plastic and viscous strains into a single component as it is practically (at the experimental level) impossible to distinguish between the two. Taking the material time derivative yields

$$\dot{\boldsymbol{\epsilon}} = \dot{\boldsymbol{\epsilon}}^e + \dot{\boldsymbol{\epsilon}}^{vp} \tag{2}$$

The time derivative of the constitutive equation for the stress is

$$\dot{\boldsymbol{\sigma}} = \mathbf{C}^e \, \dot{\boldsymbol{\epsilon}}^e \tag{3}$$

where $\dot{\boldsymbol{\sigma}}$ is the stress rate tensor and $\mathbf{C}^e$ is the elastic constitutive matrix. Note that this equation satisfies material objectivity only for small strains and small rotations.

The viscoplastic strain rate is expressed as (Perzyna, 1966)

$$\dot{\boldsymbol{\epsilon}}^{vp} = \gamma \; \phi(F) \; \frac{\partial Q}{\partial \boldsymbol{\sigma}} \tag{4}$$

where γ is a fluidity parameter with units of inverse time, ϕ is a scalar function of the yield function F and Q is a viscoplastic potential. Functions F and Q are defined later. By analogy with plasticity, the "associative viscoplasticity" is defined by $Q \equiv F$.

The <> notation implies

$$\phi(F) = \phi(F) \text{ for } F > 0 \tag{5a}$$

$$\phi(F) = 0 \text{ for } F \leq 0 \tag{5b}$$

The direction of the viscoplastic strain rate ϵ^{vp} is defined by the quantity $\partial Q/\partial\sigma$ and its magnitude is a function of the distance to the current yield surface. Figure 1 shows contours in the stress invariant plane for the function ϕ in the case of Desai's hierarchical δ model (Desai et al., 1986) and Drucker-Prager model. Here J_1 and J_{2D} are the first stress invariant and second deviatoric stress invariant, respectively. The δ-model will be used in this paper.
The most popular expressions for $\phi(F)$ are the power law

$$\phi(F) = \left[\frac{F}{F_0}\right]^N \tag{6a}$$

and the exponential law

$$\phi(F) = \exp\left[\frac{F}{F_0}\right]^N - 1 \tag{6b}$$

where N is a material parameter and F_0 a normalized constant with the same units as those of F. Other possibilities are mentioned in Vulliet and Hutter (1988).

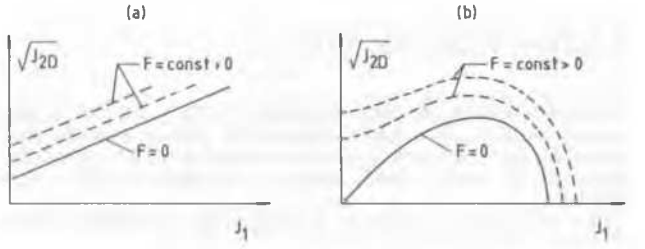

Figure 1: Contour lines of F=0 in the case of a) Drucker - Prager and b) Hierarchical δ-model (Desai et al., 1986, 1987)

Yield function

We use here the yield function F derived from the hierarchical concept (Desai et al. 1986, 1987) and given by

$$F = J_{2D} - F_b F_s \tag{7a}$$

with

$$F_b = \left[- \alpha J_1^n + \bar{\gamma} J_1^2 \right] \tag{7b}$$

$$F_s = (1 - \beta S_r)^m \tag{7c}$$

$$S_r = \frac{\sqrt{27}}{2} J_{3D} J_{2D}^{-3/2} \tag{7d}$$

n, $\bar{\gamma}$, β and m are material constants and J_{3D} is the third invariant of the deviatoric stress. α is the hardening function, one possible form being

$$\alpha = \frac{a}{(\xi_{vp})^\eta} \tag{8}$$

where a and η are hardening constants and ξ_{vp} is the trajectory of viscoplastic strain given by

$$\xi_{vp} = \int (d\epsilon_{vp}^T \, d\epsilon_{vp})^{1/2} \tag{9}$$

An other form of the hardening function α (as proposed by Desai and Hashmi, in press) is used in this paper, namely

$$\alpha = \beta_a \, e^{\zeta} \tag{10a}$$

with

$$\zeta = -\eta_1 \, \xi_{vp} \left[1 - \frac{\xi_{vp}^d}{\beta_b + \eta_2 \, \xi_{vp}^d} \right] \tag{10b}$$

where β_a, η_1, β_b and η_2 are material constants and ξ_{vp}^d is the trajectory of the deviatoric viscoplastic strain.

Viscoplastic potential

The viscoplastic potential Q in expression (4) has a form similar to the yield function F (eq. 7) except that the hardening function α is replaced by a new function α_Q that includes the nonassociative parameter κ. One possible form is:

$$\alpha_Q = \alpha + \kappa \, (\alpha_0 - \alpha) \left[1 - \frac{\xi_{vp}^v}{\xi_{vp}} \right] \tag{11}$$

where α_0 is a material constant and ξ_{vp}^v is the trajectory of the volumetric viscoplastic strains. Note that for κ=0 the model is associative.

Discussion

The viscoplastic model presented here can be characterized by the followings:

There is no time-dependent (viscoplastic) deformations if the stress state is inside of the yield surface (see eqs 4 and 5).

A state of stress outside of the yield surface will generate viscoplastic strains. This increases the amount of accumulated viscoplastic strains (ξ_{vp}), modify the value of the hardening function α and as a result change the position of the yield surface F. When F "captures" the stress point, then the displacement ceases.

Any stress point lying between the current yield surface F and the ultimate surface (given by α=0 in eq. 7b) will provoke a transient creep phenomenon. For t=∞ the result obtained by the viscoplastic model tends to the one given by the inviscid plasticity model (see Desai and Zhang 1987).

A stress point outside of the ultimate surface will provoke a secondary creep response (constant strain rate). Cormeau (1975) pointed out that in the context of limit analysis, the solution obtained when the movements stop is a lower bound while the solution obtained when the movements continue at constant rate is an upper bound.

FINITE ELEMENT SCHEME

The basic finite element scheme used here has been presented in detail in Desai and Zhang (1987). A slight modification will concern the hardening behavior and the procedure of successive iterations inside of a time-step (implicit scheme).
The viscoplastic strain rate at time n+1 is obtained by using a Taylor serie around time n as

$$\dot{\epsilon}_{vp}{}^{n+1} = \dot{\epsilon}_{vp}{}^{n} + \left[\frac{\partial \dot{\epsilon}_{vp}}{\partial \sigma}\right]^n \Delta\sigma^n + \left[\frac{\partial \dot{\epsilon}_{vp}}{\partial \xi_{vp}}\right]^n \Delta\xi_{vp}{}^n + \left[\frac{\partial \dot{\epsilon}_{vp}}{\partial \xi_{vp}{}^v}\right]^n (\Delta\xi_{vp}{}^v)^n \tag{12}$$

where $\dot{\epsilon}_{vp}{}^n$ is the viscoplastic strain rate vector at time n, $\Delta\sigma^n$ is the incremental stress vector applied at time n and $\Delta\xi_{vp}{}^n$ and $\Delta\xi_{vp}{}^{vn}$ are the induced increment of total -respectively volumetric- viscoplastic strain trajectories at time n.

The last two terms incorporate the fact that hardening occurs during a time increment. This was proposed by Marques and Owen (1982). The viscoplastic strain increment during a time interval $\Delta t^n = t^{n+1} - t^n$ is written as

$$\Delta\epsilon_{vp}{}^n = \Delta t^n \left[(1-\theta)\ \dot{\epsilon}_{vp}{}^n + \theta\ \dot{\epsilon}_{vp}{}^{n+1}\right] \tag{13}$$

For θ=0 the well known explicit Euler algorithm is obtained. It was recommanded by Cormeau (1975) as a simple and useful solution. It is however weak as far as accuracy and stability is concerned (Hughes and Taylor, 1978).

Based on numerical studies reported by Katona, Desai and Zhang (1987) recommand using θ=0.5.
Substituting (12) in (13) yields

$$\Delta\epsilon_{vp}{}^n = \Delta t^n \left[\ \dot{\epsilon}_{vp}{}^n + \theta\ \mathbf{G}^n\ \Delta\sigma^n + \theta\ \mathbf{h}^n\ \right] \tag{14}$$

with

$$\mathbf{G}^n = \left[\frac{\partial \dot{\epsilon}_{vp}}{\partial \sigma}\right]^n \tag{15a}$$

$$\mathbf{h}^n = \left[\frac{\partial \dot{\epsilon}_{vp}}{\partial \xi_{vp}}\right]^n \Delta\xi_{vp}{}^n + \left[\frac{\partial \dot{\epsilon}_{vp}}{\partial \xi_{vp}{}^v}\right]^n (\Delta\xi_{vp}{}^v)^n \tag{15b}$$

The stress increment is then evaluated from eqs. (3) and (14). Further manipulations yield

$$\Delta\sigma^n = \mathbf{C}^n \left[\Delta\epsilon^n - \Delta t^n \left[\dot{\epsilon}_{vp}{}^n + \theta\ \mathbf{h}^n\ \right]\right] \tag{16}$$

with

$$\mathbf{C}^n = (\ \mathbf{I} + \mathbf{C}^e\ \Delta t^n\ \theta\ \mathbf{G}^n\ )^{-1}\ \mathbf{C}^e \tag{17}$$

The increment of viscoplastic strain trajectories is found more easily by using Euler's rule at that stage. We then obtain

$$\Delta\xi_{vp}{}^n = \Delta t^n\ \gamma\ \phi(F)\ \left[\frac{\partial Q}{\partial \sigma}\ \frac{\partial Q}{\partial \sigma}\right]^{1/2} \tag{18a}$$

$$\Delta\xi_{vp}{}^{vn} = \Delta t^n\ \gamma\ \phi(F)\ \frac{1}{\sqrt{3}}\left[\frac{\partial Q}{\partial \sigma_{11}} + \frac{\partial Q}{\partial \sigma_{22}} + \frac{\partial Q}{\partial \sigma_{33}}\right] \tag{18b}$$

The general finite element equilibrium equation is given as

$$\int \mathbf{B}^T\ \Delta\sigma^n\ dV = \Delta\mathbf{Q}^n \tag{19}$$

where $\mathbf{B}$ is the strain-displacement matrix and $\Delta\mathbf{Q}^n$ is the vector of applied nodal loads at time n. Noting that in eq. (16) the increment of strain $\Delta\epsilon^n$ can be expressed as a function of the nodal displacements $\Delta\mathbf{q}^n$ by the equation

$$\Delta\epsilon^n = \mathbf{B}\ \Delta\mathbf{q}^n \tag{20}$$

we obtain the finite element equation as

$$\mathbf{K}^n\ \Delta\mathbf{q}^n = \Delta\bar{\mathbf{Q}}^n \tag{21}$$

where

$$\Delta\bar{\mathbf{Q}}^n = \Delta\mathbf{Q}^n + \int \mathbf{B}^T\ \mathbf{C}^n\ \Delta t^n \left[\dot{\epsilon}_{vp}{}^n + \theta\mathbf{h}^n\right] dV \tag{22a}$$

$$\mathbf{K}^n = \int \mathbf{B}^T\ \mathbf{C}^n\ \mathbf{B}\ dV \tag{22b}$$

It is evident from (21) that this formulation is very similar to the one of inviscid plasticity. The only difference is in the form of the constitutive matrix $\mathbf{C}$ (replaced by $\mathbf{C}^{ep}$ in plasticity) and the modified load vector ($\Delta\bar{\mathbf{Q}}^n \neq \Delta\mathbf{Q}^n$).

Algorithm

The preceding equations contain all the necessary ingredients to compute the strains and stresses at time n when these quantities are known at time n-1. This step will be called iteration 0. We will then show how to improve the solution at time n by successive iterations.

Iteration 0

1. Solve $\mathbf{K}_0{}^n\ \Delta\mathbf{q}_0{}^n = \Delta\bar{\mathbf{Q}}_0{}^n$
2. Compute $\Delta\epsilon_0{}^n = \mathbf{B}\ \Delta\mathbf{q}_0{}^n$
3. Compute $\Delta\sigma_0{}^n$ with eq. (16)
4. Update $\sigma_0{}^n = \sigma_i{}^{n-1} + \Delta\sigma_0{}^n$

The solution $\Delta\mathbf{q}_0{}^n$ $\Delta\sigma_0{}^n$ can be improved by successive iterations inside of the time-step n. An improved solution is written as:

$$\begin{aligned}\Delta\sigma_1{}^n &= \Delta\sigma_0{}^n + \Delta\Delta\sigma_0{}^n \\ \Delta\mathbf{q}_1{}^n &= \Delta\mathbf{q}_0{}^n + \Delta\Delta\mathbf{q}_0{}^n\end{aligned} \tag{23}$$

The first terms of the right hand side are known from the iteration 0. By posing:

$$\dot{\epsilon}_{vp1}{}^n = \dot{\epsilon}_{vp0}{}^n + \mathbf{G}_0{}^n\ \Delta\Delta\sigma_0{}^n \tag{24a}$$

$$\mathbf{G}_1{}^n = \mathbf{G}_0{}^n \text{ (Euler's assumption)} \tag{24b}$$

and taking $\Delta\Delta\sigma_0{}^n$ from eq. (23a) we obtain, after manipulations, the following procedure for the first iteration:

Iteration 1

1. Solve $\bar{\mathbf{K}}_0{}^n\ \Delta\Delta\mathbf{q}_0{}^n = \Delta\mathbf{Q}^n - \int \mathbf{B}^T\ \Delta\sigma_0{}^n\ dV$

   with $\bar{\mathbf{K}} = \int \mathbf{B}^T\ \bar{\mathbf{C}}_0{}^n\ \mathbf{B}\ dV$

   and $\bar{\mathbf{C}}_0{}^n = (\ \mathbf{I} + \mathbf{C}^e\ \Delta t^n\ (1+\theta)\ \mathbf{G}_0{}^n\ )^{-1}\ \mathbf{C}^e$
2. Compute $\Delta\Delta\epsilon_0{}^n = \mathbf{B}\ \Delta\Delta\mathbf{q}_0{}^n$

3. Compute $\Delta\Delta\sigma_0^n = \bar{C}_0^n \, \Delta\Delta\epsilon_0^n$

4. Update $\Delta\sigma_1^n = \Delta\sigma_0^n + \Delta\Delta\sigma_0^n$

This procedure can be simplified and the computer time costs reduced if, as an approximation, the stiffness matrix $\mathbf{K}$ is not updated during the iterations ($\bar{\mathbf{K}} \equiv \mathbf{K}$).

Iteration i

Repeat the above steps with the new indices i for 1 and i-1 for 0. The iterations are stopped when a specified convergence criterion is satisfied or after a given number of iterations.

EXAMPLES

Isotropic compression

Fig. 2 shows the result of an hydrostatic compression test on an axisymmetric specimen shown in the figure. The finite element mesh consists of four 8-nodes isoparametric elements with boundary conditions as shown on the figure. The isotropic stress applied is $\sigma_1 = \sigma_2 = \sigma_3 = 91.4$ kPa (13 psi). The material is characterized by the following constants: E = 75790 kPa (11000 psi); ν = 0.29; $\bar{\gamma}$ = 0.4595; β = 0.3624; m = -0.5; n = 2.5; β_a = 0.0351; η_1 = 450; κ = 0.29; α_0 = 0.013; β_b = 1.02; η_2 = 0.0047.

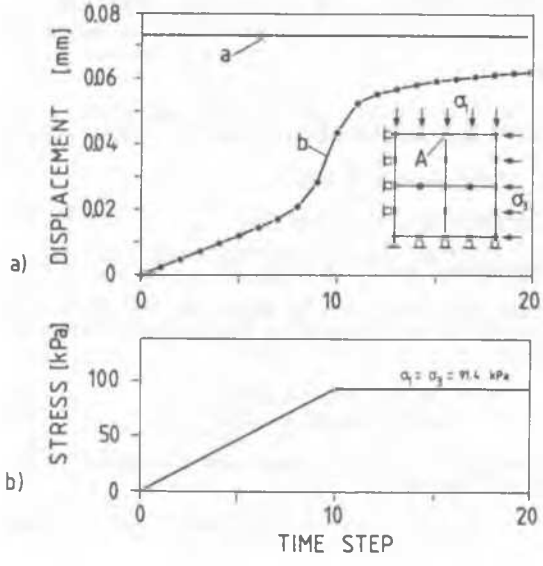

Figure 2: Isotropic compression test. a) Vertical displacement of point A as a function of time; b) imposed boundary-stress history

The solid line (a) in figure 2 represents the vertical displacement of the point A shown on the mesh when the plastic model is used. The curve (b) represents the displacement as a function of time for the same point A when the viscoplastic model is used with the power law (eq. 5a) and the following constants: $\gamma = 10^{-9}$ T^{-1}; N = 3; F_0 = 1.0; Δt = const = 0.01 T; θ = 0.5 (note that T stands for any time units). The load history is given in figure 2b.

It can be seen that the viscoplastic solution converges toward the plastic solution. Further, during the period of constant load (starting at time-step 10) the movement is the one of a "primary creep" (with decreasing strain rate) as described in the discussion above.

Conventional triaxial compression

In this example, the same specimen (same material) is subjected to a different load history. An isotropic load is first applied (same as above), and then the vertical load is increased ($\Delta\sigma_1$ = 372.6 kPa (53 psi)) while keeping the horizontal load constant ($\Delta\sigma_2 = \Delta\sigma_3 = 0$), corresponding to a conventional triaxial compression test ($\sigma_1 > \sigma_2 = \sigma_3$).

Figure 3a contains results from plastic and viscoplastic analysis. The solid line (a) shows the vertical displacement of point A (as before) for the plastic (time independent) analysis. The other curves correspond to different viscoplastic analysis induced by the load history shown in figure 3b.

Curve (b) is obtained using the previously defined viscoplastic parameters and no iteration within a time step; the solution is unstable. This is because of the use of a large time-step. When this procedure is used (no iterations), the length of the time-step must be controlled in order to guaranty stability (see Marques and Owen 1983).

Curve (c) is obtained with 2 iterations and curve (d) with 5 and 10 iterations. These solutions are stable but not necessarily accurate. The accuracy can be improved in reducing the size of the time-step. This was done for curve (e) where the time-step is one half of the previous one (Δt = const = 0.005 T).

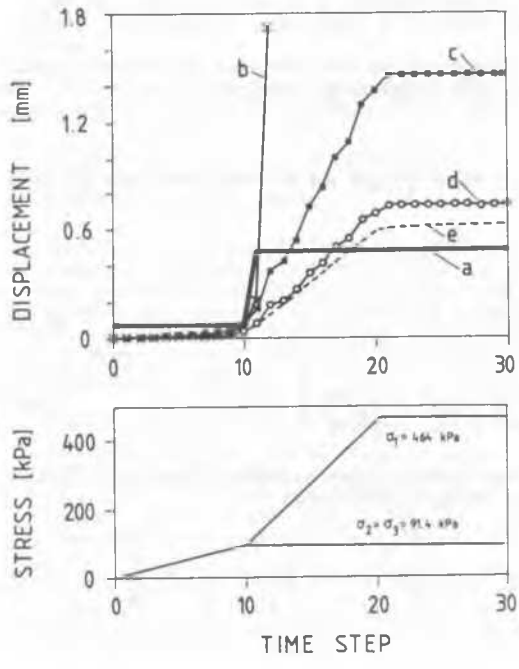

Figure 3: Triaxial compression test. a) Vertical displacement of point A (see Fig. 2) with time for different assumptions; b) imposed boundary-stress history

La Frasse landslide

The La Frasse landslide lies in the Swiss Alps, 60 km east of Lausanne. It covers an area 2000 m long by 400 m wide; it is about 60 m thick and has a mean slope angle of approximately 13° . The long term sliding velocities are between 10 and 50 cm/year. This site is described in Vulliet and Hutter (1988b) where a viscous 3D analysis with finite differences is presented. Here we will perform a 2D visco*plastic* analysis using the proposed finite element formulation and compare the results of the two approaches.

The finite element mesh is presented in Figure 4. It consists of 132 isoparametric eight-nodes elements and a total of 491 nodes. Note that in the figure the vertical and horizontal scales are different.

As in Vulliet and Hutter (1988b), the groundwater level is assumed to coincide with the free ground surface. This assumption comes from field observations and is not a limitation of the numerical model.

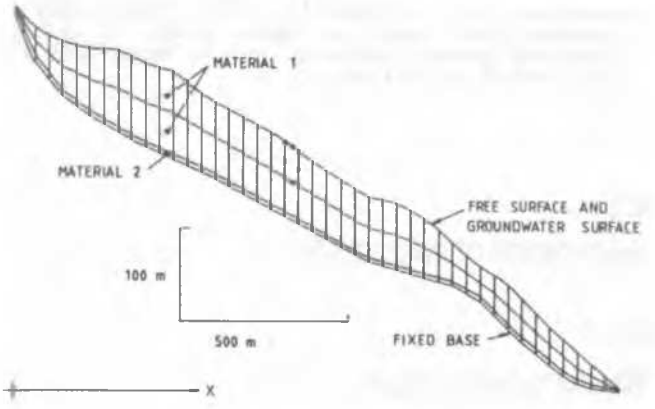

Figure 4: Finite element mesh for the "La Frasse" landslide

The displacement of the soil mass is characterized by strong shear deformations in the vicinity of the sliding surface (or base) of the landslide, and a solid-body type of motion for the upper sliding mass. As a consequence, two materials are considered. Material 1 represents the sliding mass and material 2 the -weaker- sliding surface zone. For this analysis the sliding surface zone is represented by thin solid elements (effective thickness of 5 m) but interface elements could have been used as well (e.g. the thin-layer elements, Desai et al. 1984)

The material parameters are shown in Table I. Assuming that the angle of internal friction is the same for both triaxial compression and extension test, that is $\phi_C = \phi_E = 12^o$ for the material 2 (interface), we find the parameters β and $\bar{\gamma}$ following Desai and Wathugala (1987):

$$\beta = \frac{1 - \left[\frac{\tan\theta_C}{\tan\theta_E}\right]^{\frac{2}{m}}}{1 + \left[\frac{\tan\theta_C}{\tan\theta_E}\right]^{\frac{2}{m}}} \quad \text{and} \quad \sqrt{\bar{\gamma}} = \frac{\tan\theta_C}{(1-\beta)^{\frac{1}{m}}} \qquad (25)$$

with

$$\tan\theta_C = \frac{2\sin\phi_C}{\sqrt{3}\,(3 - \sin\phi_C)} \qquad (26a)$$

$$\tan\theta_E = \frac{2\sin\phi_E}{\sqrt{3}\,(3 + \sin\phi_E)} \qquad (26b)$$

For the sliding mass the angle of internal friction is taken as $\phi_C = \phi_E = 25^o$ and equations (25) and (26) determine the values of β and $\bar{\gamma}$ given in Table I.

As no data are available concerning the hardening behavior, the hardening function α is taken as $\alpha \equiv 0$ with $\beta_a = 0$ in eq. (10a). As a consequence the values of n, η_1, η_2 and β_b are chosen for computational purpose only and their actual values will depend on (laboratory) test data; this aspect is being studied. Note that even with this simplification the δ-model is different from the Drucker-Prager model because β in eq. (7c) is not equal to zero (in the π-plane the yield surface is not a circle).

For the same reason of lack of test data at this time we will assume that the flow rule is associative, that is $\kappa = 0$ in eq. (11). The power law (eq. 6a) is assumed for viscous strains with values given in Table I; they are derived from the previous analysis by Vulliet and Hutter(1988b).

Table I. Parameters used for La Frasse. a) Material parameters and b) time integration parameters.

	Parameter	Value Mat. 1	Mat. 2	Units
a)	E	79200	same	kPa
	ν	0.29	same	-
	$\bar{\gamma}$	0.025	$6.313\ 10^{-3}$	-
	β	0.513	0.2707	-
	m	-0.5	same	-
	β_a	0	same	-
	κ	0	same	-
	γ	$4.34\ 10^{11}$	same	s^{-1}
	N	2	same	-
	F_0	10^5	same	$(kPa)^2$
b)	Δt	$2.7\ 10^6$		s
	θ	0.5		-

The results are presented in Figure 5. The solid dots represent long term velocity measurements. Curve a) corresponds to the present analysis; the plotted velocities represent long term conditions after application of in-situ stresses. Curve b) is taken from the viscous analysis by Vulliet and Hutter.

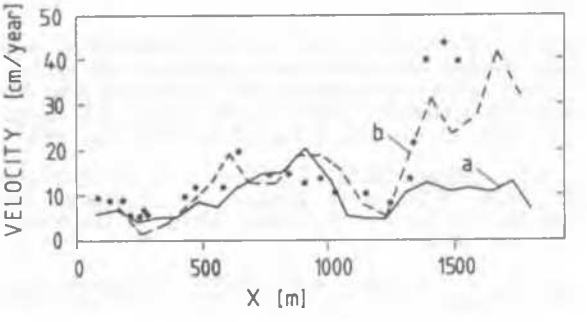

Figure 5: Longitudinal velocity distribution for "La Frasse". Comparison between measured values (full dots), present analysis (curve a) and previous analysis by Vulliet and Hutter 1988b (curve b)

It can be seen that the results are consistent with measured data and previous viscous analysis. In the lower part of the landslide (x>1500 m) the analysis underestimates the velocities. This is due to the fact that identical material parameters have been used along the entire sliding surface. In situ tests have shown that the material in the lower part is weaker than in the upper part. Moreover, due to the complex geology of the region, the lower part of the landslide is experiencing artesian water pressures that are not considered in this analysis. Fine tuning of the model will allow for a better simulation (back-prediction) of the real behavior and then an evaluation of remedial measures as drainage, anchors or retaining structures.

CONCLUSION

The presented finite element scheme is considered to be stable and accurate. The viscoplastic approach can be used for example for analyzing time-dependent slope deformations; the formulation is such that inhomogeneities and local effects like anchors or retaining walls can be incorporated, what was not possible in the previous dimensional analysis by Vulliet and Hutter. Some of the future improvements being considered are (1) material constants based on laboratory tests for the soil and interface zone and (2) incorporation of large displacements.

ACKNOWLEDGEMENTS

This work was supported by the Swiss NSF, grant 82.480.0.87. The authors are thankful to this organization.

REFERENCES

Cormeau, I. (1975). Numerical stability in quasi-static elasto-viscoplasticity. Int. J. Num. Meth. in Eng., Vol. 9, pp. 109-127

Desai, C.S., Hashmi, Q.S.E. Analysis, evaluation and implementation of a nonassociative model for geologic materials. Int. J. of Plasticity, in press

Desai, C.S., Somasundaram,S. and Frantziskonis, G. (1986). A hierarchical approach for constitutive modelling of geologic materials. Int. J. Num. Analyt. Meth. in Geomech., Vol 10, No 3, pp. 225-258

Desai, C.S., Zhang, D. (1987). Viscoplastic model for geologic materials with generalized flow rule. Int. J. Num. Analyt. Meth. in Geomech., Vol.11, No.6, pp. 603-620

Desai, C.S., Wathugala, G.W. (1987). Hierarchical and unified models for solids and discontinuities (joints, interfaces). in: Implementation of constitutive laws for engineering materials - short course notes, C.S. Desai editor, Univ. of Arizona, Tucson USA 9-10 Jan. 1987

Desai, C.S., Zaman, M.M., Lightner, J.G., Siriwardane, H.J. (1984). Thin-layer element for interfaces and joints. Int. J. Num. and Analyt. Meth. in Geomech., Vol. 8, pp. 19-43

Hugues, T.J.R., Taylor, R.L. (1978). Unconditionally stable algorithms for quasi-static elasto-visco-plastic finite element analysis. Computers and Structures, Vol. 8, pp. 169-173

Inoue, T. (1987). Inelastic constitutive laws under plasticity and creep interaction condition - Theories and evaluations. in: Implementation of constitutive laws for engineering materials - short course notes, C.S. Desai editor, Univ. of Arizona, Tucson, USA, 9-10 Jan. 1987

Marques, J.M.M.C., Owen, D.R.J. (1983). Strain hardening representation for implicit quasistatic elasto-viscoplastic algorithms. Computers and Structures, Vol. 17, No. 2, pp. 301-304

Perzyna, P. (1966). Fundamental problems in viscoplasticity. Advances in Applied Mechanics, Academic Press, New York, Vol 9, pp. 244-368

Valanis, K.C. (1971). A theory of viscoplasticity without a yield surface. Archives of Mech., No 23, pp. 517-555

Vulliet, L., Hutter, K. (1988a). Some constitutive laws for creeping soil and for rate-dependent sliding at interfaces. Int. Conf. on Num. Meth. in Geomech., Insbruck (Austria), Vol.1, pp. 495-502

Vulliet, L., Hutter, K. (1988b). Continuum model for natural slopes in slow movement. Geotechnique, Vol. 38, No. 2, pp. 199-218

Zienkiewicz, O.C., Cormeau, I.C. (1974). Visco-plasticity, plasticity and creep in elastic solids: a unified numerical solution approach. Int. J. Num. Meth. in Eng., Vol. 8, pp. 821-845